Cytoplasmic Dynein-like ATPase Cross-links Microtubules in an ATP-sensitive Manner

PETER J. HOLLENBECK, FRANK SUPRYNOWICZ, and W. ZACHEUS CANDE
Department of Botany, University of California at Berkeley, Berkeley, California 94720. Dr. Suprynowicz's present address is Hopkins Marine Station, Pacific Grove, California 93950.

ABSTRACT We have prepared dynein-like ATPase from the eggs of the sea urchin *Strongylocentrotus purpuratus* using differential centrifugation and column chromatography. This ATPase preparation is inhibited by vanadate and erythro-9-(3-[2-hydroxynonyl]) adenine (EHNA) at concentrations similar to those that inhibit reactivated flagellar beating and spindle elongation in lysed cell models. Using microtubule affinity and ATP-induced release, we can purify this ATPase activity to a composition on SDS PAGE of four peptides ranging in molecular weight from 180,000–300,000. When viewed in darkfield optics, this affinity-purified ATPase caused extensive parallel bundling of microtubule-associated protein–free microtubules. These bundles were dispersed by 1 mM ATP but not by ATPγS or AMP-5′-adenylimidodiphosphate. The reformation of microtubule bundles after dispersal by ATP required ATP hydrolysis; bundles did not reform in the presence of 10 μM vanadate. Negative stain electron microscopy of these bundled microtubules revealed that they are arranged in parallel networks with extensive close lateral association.

Microtubule systems are often organized into orderly arrays by lateral interactions between tubules. In many cases, these lateral interactions are mediated by cross-bridges that can be seen in the electron microscope or purified and characterized biochemically. Such systems include the ciliary or flagellar axoneme (12, 42, 48, 52, 53, 56), the protozoan axostyle (2, 3, 17), the pharyngeal basket of certain ciliates (51), the heliozoan axopod (50), and the mitotic apparatus (20, 27, 28). While some cross-bridges may merely be static links others are likely to generate force for microtubule-based movements. Of these systems, only one, the axoneme, has had its cross-bridging elements characterized both morphologically and biochemically. They consist of both static bridges such as the nexin links and the mechanochemical protein, dynein.

While the mitotic apparatus lacks the order of the axoneme, it has been suggested that a dynein-like cross-bridge plays a role in its formation and function, and particularly in anaphase chromosome movement. Two kinds of studies have provided evidence for this view. First, morphological studies of diatoms reveal a highly ordered spindle midzone in which microtubules from opposite half-spindles interdigitate in a regular array. The distance between nearest neighbor microtubules in this midzone is appropriate for dynein cross-bridging, and in some preparations arms or bridges can be seen projecting from most of the microtubules in the midzone (27, 28).

A second line of evidence for dynein involvement in anaphase comes from physiological studies using permeabilized PtK1 cell spindle models. These models, which permit the study of anaphase under controlled conditions, have shown that separation of the spindle poles requires ATP and is inhibited by vanadate and erythro-9-(3-[2-hydroxynonyl]) adenine (EHNA)[1] (6, 7) which are both potent inhibitors of dynein ATPase activity (23, 34). In addition, it has been reported that isolated sea urchin embryo mitotic spindles move chromosomes and that this movement is blocked by vanadate and antibodies to flagellar dynein (40).

If a dynein ATPase is a component of the mitotic apparatus, then it should be identifiable in preparations of mitotic apparatuses or cytoplasm. A MgATPase activity was originally reported in isolated spindles of the sea urchin egg by Mazia et al. (26). Weisenberg and Taylor (55) suggested that this ATPase was a precursor to embryonic ciliary dynein bound nonspecifically to spindle preparations, but subsequent work

[1] *Abbreviations used in this paper.* AMPPNP, 5′-adenylimidodiphosphate; EHNA, erythro-9-(3-[2-hydroxynonyl]); MAP, microtubule-associated protein; PME, 100 mM PIPES, 1 mM $MgSO_4$, 1 mM EGTA.

THE JOURNAL OF CELL BIOLOGY · VOLUME 99 OCTOBER 1984 1251–1258

by Pratt (36, 37, 39) made this seem unlikely, as did the claim of Pallini et al. (32) of having isolated similar dynein-like ATPases from cells that do not give rise to cilia (32).

A dynein-like ATPase has now been prepared and characterized from the mitotic apparatuses and cytoplasm of sea urchin embryos by several investigators (21, 33, 38). It has the high sedimentation coefficient, high molecular weight gel bands, and Mg^{++} and Ca^{++} activation expected for dynein, and it shows inhibition by vanadate and EHNA. But these are not the only properties of dynein critical to a role in mitosis and other microtubule-based movements. To be a likely candidate for involvement in these processes, this ATPase must bind to and cross-link microtubules. Recent work by Hisanaga and Sakai (22) addressed this question using an ATPase preparation purified to a single high molecular weight polypeptide. As judged by gels, this polypeptide pelleted with microtubules in an ATP-sensitive manner. Binding of the ATPase activity to microtubules was not measured directly, but activity disappeared from the supernatant when microtubules were pelleted.

In this study, we prepared cytoplasmic dynein-like ATPase from sea urchin eggs by size filtration chromatography followed by microtubule affinity and ATP-induced release. We used dark-field optics and negative stain electron microscopy to demonstrate the microtubule cross-linking properties of this preparation and to correlate its cross-linking activity with its ATPase activity.

MATERIALS AND METHODS

Cytoplasmic Dynein-like ATPase Preparation: Sea urchins of the species *Strongylocentrotus purpuratus* were spawned by filling the coelom with 0.5 M KCl. Eggs were collected in filtered natural sea water, dejellied by passage through 190-μm nitex mesh, and washed twice with filtered natural sea water. After one washing with gluconate buffer (10 mM HEPES, 0.3 M potassium gluconate, 0.33 M glycine, 10 mM NaCl, 5 mM $MgSO_4$, 1 mM EGTA, pH 7.4), eggs were resuspended in 3 vol of the same buffer at 4°C containing 0.5% protease inhibitor stock (0.2 mg/ml leupeptin, 2 mg/ml soybean trypsin inhibitor, 0.2 mg/ml pepstatin A, 2 mg/ml *N*-α-benzoyl-L-arginine methyl ester, 2 mg/ml *p*-tosyl-L-arginine methyl ester, 2 mg/ml L-1 tosylamide-2-phenylethylchloromethyl ketone) and disrupted by 15 strokes with a glass Dounce hand homogenizer. The cell homogenate was centrifuged at 40,000 *g* for 30 min at 4°C and the supernatant was carefully removed and further centrifuged at 125,000 *g* for 75 min at 4°C. The resulting high speed supernatant was concentrated by ammonium sulfate precipitation at 40% saturation. Precipitated protein was resuspended in HE buffer (10 mM HEPES, 0.1 mM EDTA, pH 7.4) containing 0.5 mM α-mercaptoethanol and 0.2% protease inhibitor stock and dialyzed three times at 4°C against 150 vol of the same buffer, three h per change. The dialysate was clarified by centrifugation at 125,000 *g* for 60 min at 4°C. The resulting supernatant was loaded onto a 2.6 × 80 cm Bio-Gel A15m sizing column equilibrated in HE buffer plus 0.6 M KCl and 0.2% protease inhibitor stock. This column was run at 2–4°C at a linear flow rate of 6 cm/h and 7.5-ml fractions were collected. MgATPase activity eluted in a peak with K_{av} of 0.3–0.5 (Fig. 1). The peak fractions were pooled and dialyzed twice at 4°C against 100 vol of 50 mM PIPES, 1 mM $MgSO_4$, 1 mM EGTA (PME), and 0.2% protease inhibitor stock, pH 6.94. It was then clarified by spinning at 125,000 *g* for 60 min. This pooled, dialyzed, clarified peak was then used to dilute DEAE-purified tubulin to a tubulin concentration of 1.6–2.0 mg/ml. The tubulin was polymerized into microtubules by addition of taxol equimolar with tubulin dimers and the microtubules were pelleted at 125,000 *g* for 45 min at 4°C. The resulting microtubule pellet was resuspended to a concentration of 10 mg/ml in PME plus 2 mM MgATP and pelleted again at 125,000 *g* for 45 min. This process was repeated with the second pellet and the supernatants were combined. These supernatants contained MgATPase activity.

Tubulin Preparation: Twice-cycled microtubule protein was prepared by the method of Shelanski et al. (45) and stored at −80°C. Tubulin was purified from this preparation by ion exchange chromatography on DEAE-Sephadex after the method of Murphy and Borisy (31) and dialyzed against 200 vol of PME plus 0.1 mM GTP for 60 min.

ATPase Activity Assays and Protein Determinations: Material was assayed for ATPase activity by incubation at 25°C in 100 mM Tris HCl, pH 8.0, 100 mM KCl, 5 mM $MgSO_4$ or $CaCl_2$, 1 mM EGTA, and 2 mM ATP for 18 min. (When assaying in the presence of EHNA, ATP was adjusted to 10% of the EHNA concentration.) Samples were withdrawn from the incubation mixture every 3 min from 6 through 18 min and assayed for inorganic phosphate after the method of Fiske and Subbarow (9). Vanadate was prepared for inhibition studies by making a 1-mM stock solution of sodium orthovanadate (Na_3VO_4) in distilled H_2O and placing it briefly in a boiling water bath. This stock was prepared fresh each day.

The K_m for ATP was determined by assaying the sizing column peak fraction at ATP concentrations ranging from 0.1 to 4 mM. The data was analyzed using Eadie-Hofstee plots and gave straight lines with correlation coefficients of <-0.996. Samples were assayed for protein by the method of Bradford (4), using BSA as a standard.

Microtubule Pelleting Binding Assay: Microtubules were prepared by polymerizing DEAE-purified tubulin with taxol. Column-enriched ATPase was combined with microtubules and incubated in the presence of no Mg^{++}, 5 mM $MgSO_4$, or 5 mM $MgSO_4$ + 0.5 mM ATP for 30 min. Incubation mixtures were then layered over a pad of 3 vol of 20% sucrose in HE buffer containing the same cation and/or nucleotide concentration as the incubation mixture and 0.2% protease inhibitor stock. They were centrifuged in an SW50.1 rotor (Beckman Instruments, Inc., Palo Alto, CA) at 125,000 *g* for 60 min at 4°C and pellets were assayed for ATPase activity. As controls, either microtubules or ATPase alone was layered over pads and centrifuged.

Darkfield Microscopy: Microtubule-associated protein (MAP)-free taxol-stabilized microtubules were diluted to 0.2 mg/ml with PME or microtubule affinity-purified ATPase. In the latter case, this resulted in a ratio of 0.4 mg nontubulin peptides/1 mg microtubules. These mixtures were incubated under various ionic and nucleotide conditions and viewed after 5 and 30 min. Glass slides were thoroughly rinsed with Millipore-filtered (Millipore Corp., Bedford, MA) distilled water and dried by air jet. Samples of 1–2 μl were placed on these slides and covered with air dusted coverslips. Slides were viewed using a Zeiss dark-field condensor and a Zeiss 100× plan objective with an iris. Photographs of typical fields were taken with Kodak Tri-X film at ASA 1600.

Electron Microscopy: Samples of microtubules or microtubules plus ATPase were removed from the dark-field assay mixtures and applied to Formvar-coated grids. After 10 s, the samples were drawn off and the grids were prepared by floating them upside down on a series of solutions after the method of Langford (25): 5 s each on two changes of PME, 30–60 s on PME plus 0.1% glutaraldehyde, 5 s each on two changes of PME, 5 s each on two changes of distilled H_2O, 5 s each on four changes of bacitracin (40 μg/ml in distilled H_2O), excess liquid was drawn off, then 5 s each on three changes of aqueous 1% uranyl acetate. Excess stain was drawn off and grids were allowed to air dry. Grids were viewed with a Zeiss EM 109.

Gel Electrophoresis: Samples were denatured and run on 4–8% polyacrylamide gradient gels made after the method of Laemmli (24). These were stained with Coomassie Blue and stored in 10% acetic acid. Gels were photographed with Kodak Pan-X film.

Molecular weight determinations were made using standard proteins of molecular weights 45,000, 66,200, 92,500, 116,250, and 200,000. In this gel system, the molecular weights and R_f values of these standards have a nearly perfect linear relationship, with a correlation coefficient of <-0.999.

Stained gels were scanned with a densitometer (E-C Apparatus Corp., St. Petersburg, FL) with a 570-nm filter. The percent of total protein in each band was assumed to be proportional to the percent of the total area under its curve.

RESULTS

Purification and Enzymatic Properties of Cytoplasmic Dynein-like ATPase

We prepared dynein-like ATPase from sea urchin eggs using a protocol that exploits its high molecular weight and microtubule-binding properties. Differential centrifugation, ammonium sulfate precipitation, and size filtration (Figs. 1 and 2) provided a rapid 40-fold enrichment of MgATPase activity with a 15% recovery (Table I). When assayed under various conditions (Table II), this column-enriched ATPase showed cationic requirements and oligomycin and ouabain insensitivity similar to dynein-like ATPase prepared in different ways by other investigators (21, 33, 37). In addition, it was inhibited by EHNA in a concentration range very similar to that found for dynein-like ATPase from urchin eggs by Penningroth and

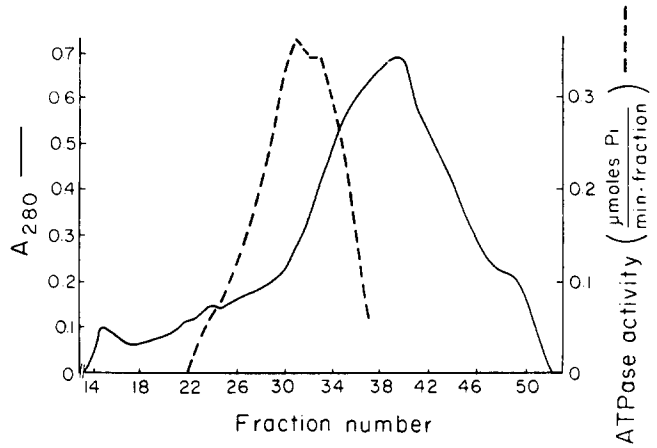

FIGURE 1 Elution profile of cytoplasmic dynein MgATPase on a sizing column. The clarified dialyzed ammonium sulfate fraction was subjected to gel filtration on a 2.6 × 80-cm column of Bio-Gel A15m equilibrated and eluted with 0.6 M KCl, 10 mM HEPES/KOH, 0.1 mM EDTA, 0.5 mM α-mercaptoethanol, and 0.2% protease inhibitor stock, pH 7.4. It was run at 2–4°C at a linear flow rate of 6 cm/h and 7.5-ml fractions were collected and assayed for absorbance at 280 nm and MgATPase activity as described in Materials and Methods. The activity eluted in a peak with K_{av} of 0.3–0.5.

Cheung (33) and from brain by Pallini et al. (32). However, our ATPase preparation was more sensitive to vanadate inhibition than those reported by other workers, with our half-inhibitory concentration (1 μM) as much as 10-fold lower than reported values. This may be due to the relative heterogeneity of their preparations, or to the presence in their stocks of vanadate not in the +5 oxidation state. Assays with other nucleotides (Table II) showed that the Mg-stimulated activity was relatively ATP specific. The K_m of the column-enriched ATPase for ATP was 66 μM under our assay conditions.

The MgATPase was further purified from the column-enriched fraction by a microtubule affinity and ATP-induced release procedure. When taxol-polymerized brain microtubules were incubated with this column-enriched ATPase and then pelleted, 75% of the MgATPase activity pelleted with them. When these pellets were extracted with 2 mM MgATP and repelleted, they released 25–35% of the activity to the supernatant. When examined on 4–8% gradient SDS polyacrylamide gels, this ATP-released ATPase preparation revealed only four major peptides along with tubulin extracted from the microtubules (Fig. 2, lane *D*). This extraction of tubulin was due to the slight lability of taxol-polymerized microtubules in the cold. The nontubulin peptides had M_r values of 295,000, 246,000, 243,000, and 180,000. The presence of soluble tubulin in the supernatant necessitated the use of densitometry of gel lanes to determine the percentage of nontubulin peptides there. Densitometry indicated that the four nontubulin peptides composed 3.6% of the protein in the ATP-released supernatant while tubulin composed the rest. This allowed the calculation of an estimated specific ATPase activity for these peptides of 0.850 μmoles P_i/min per mg protein.

Pelleting ATPase Assay

In the presence of 5 mM Mg^{++}, 32% of the ATPase activity incubated with microtubules pelleted with them through the sucrose pad. In the absence of Mg^{++}, this was reduced to 9.5%, while in the presence of 5 mM Mg^{++} and 0.5 mM ATP,

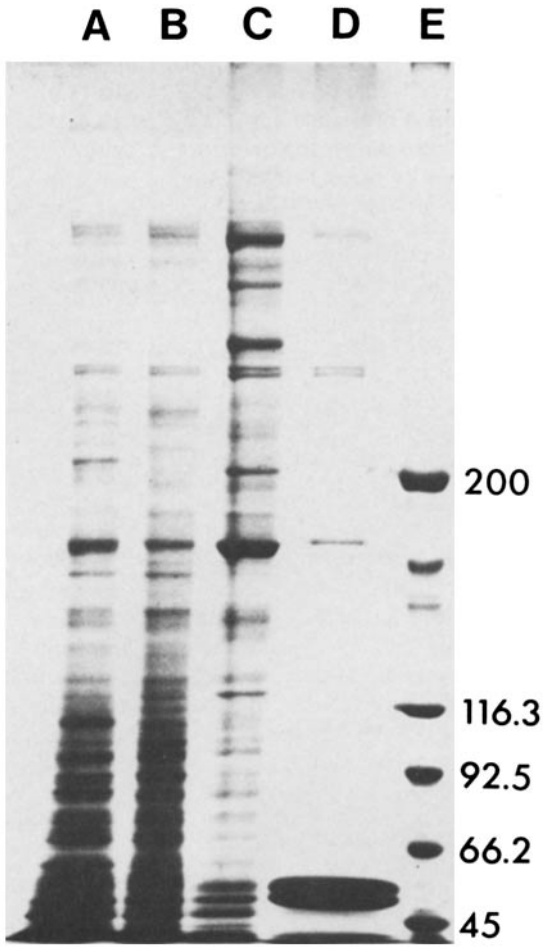

FIGURE 2 SDS PAGE of fractions from the purification procedure using a 4–8% gradient gel. Lanes *A–D* contain 20 μg each of (*A*) high speed cytoplasmic supernatant; (*B*) clarified dialyzed 40% ammonium sulfate fraction; (*C*) Bio-Gel A15m column peak fraction; (*D*) fraction released from microtubule binding by ATP. Lane *E* contains molecular weight standards: myosin (200,000); β-galactosidase (116,300); phosphorylase *b* (92,500); BSA (66,200); and ovalbumin (45,000).

TABLE I
Purification of Dynein-like ATPase

Fraction	Total protein	Total MgATPase activity	Specific activity	Enrichment for each step
	mg			
Homogenate	1,500	7.5	0.005	—
S125	300	5.2	0.017	3.4×
cdAMS	107	4.3	0.040	2.3×
Column peak	5.5	1.1	0.200	5.0×
Mt affinity	0.35	.30	0.850	4.5×

S125, high speed supernatant of cytoplasmic homogenate; *cdAMS*, clarified dialyzed 40% ammonium sulfate fraction of S125; *column peak*, MgATPase peak from Bio-Gel A15m sizing column; *Mt affinity*, fraction released from binding to microtubules by ATP. All fractions were assayed for ATPase in 100 mM Tris/HCl, pH 8.0, 100 mM KCl, 5 mM $MgSO_4$, and 2 mM ATP. Homogenate was assayed in the presence of 10 μg/ml of oligomycin. Total MgATPase activity is expressed in micromoles inorganic phosphate per minute and specific activity is expressed in micromoles inorganic phosphate per (minute × milligram protein). Total protein and specific activity of the microtubule affinity fraction are adjusted for nontubulin peptides only as determined by densitometric measurements of this fraction on SDS gels.

14% of the activity pelleted. In the absence of microtubules, no detectable activity pelleted.

Characterization of ATPase/Microtubule Interactions by Darkfield Optics

Microtubules polymerized from purified tubulin and diluted to 0.2 mg/ml with PME were visible in dark-field microscopy as bright individual filaments distributed evenly across the field (Fig. 3*A*). When these microtubules were diluted to 0.2 mg/ml with affinity-purified ATPase in the presence of 5 mM Mg^{++}, the dark-field image was dramatically different (Fig. 3*B*). Essentially all of the microtubules in the field were seen to be gathered into bright dense bundles, with individual microtubules apparent at the edges.

The addition of 1 mM MgATP to microtubules so bundled (Fig. 4*A*) resulted in their complete dissociation within 5 min into scattered individual microtubules (Fig. 4*B*). After an interval sufficient to allow complete hydrolysis of ATP by the ATPase (30 min), microtubules again appeared in bundles (Fig. 4*C*). However, when 1 mM ATP + 10 μM vanadate were added, the bundles (Fig. 4*D*) dispersed but failed to form again over a period of 60 min (Fig. 4, *E* and *F*). The addition of 1 mM ATPγS or 1 mM AMP-5′-adenylimidodiphosphate (PNP) to microtubules bundled by the ATPase (Fig. 4, *G* and *J*) resulted in very little dispersal of the bundles (Fig. 4, *H*, *I*, *K*, and *L*).

In the absence of Mg^{++}, incubation of microtubules with ATPase did not result in any visible bundling of microtubules. Likewise, the addition of Mg^{++} to microtubules without ATPase gave no bundling. When the dark-field assays described above were performed with sizing column-enriched ATPase rather than affinity-purified material, the results were essentially the same (data not shown).

TABLE II

Nucleoside Triphosphatase Activities

Assay conditions	Control ATPase activity
	%
2 mM ATP, 5 mM $MgSO_4$	100
+10 μg/ml oligomycin	103
+0.1 mM ouabain	102
+0.5 μM vanadate	76
+1.0 μM vanadate	54
+2.0 μM vanadate	0
+1 mM EHNA	46
+2 mM EHNA	0
2 mM GTP	6
2 mM ITP	6
2 mM CTP	15
2 mM ATP, 5 mM $CaCl_2$	83

All assays were performed using sizing column peak fractions as described in Materials and Methods.

Negative Stain Electron Microscopy

To observe the fine structure of microtubules bundled by the ATPase, we prepared samples of the dark-field incubation mixtures for electron microscopy. Microtubules alone showed fairly typical negative stain morphology, appearing long and straight with excellent resolution of protofilaments and individual dimers (Fig. 5, *A* and *B*). The microtubules were free and unassociated and were distributed evenly across the grid. But microtubules incubated with dynein-like ATPase in the presence of Mg^{++} were gathered into parallel bundles of various size. Within these bundles, microtubules ran parallel to one another and were frequently separated by a gap of 5–20 nm. Also, globular structures were seen along some microtubules, but no stretches of periodic decoration were observed (Fig. 5, *C* and *D*).

DISCUSSION

In the search for a dynein-like ATPase that might be involved in anaphase chromosome movement, we must ask ourselves two questions: first, is there a candidate ATPase in the cyto-

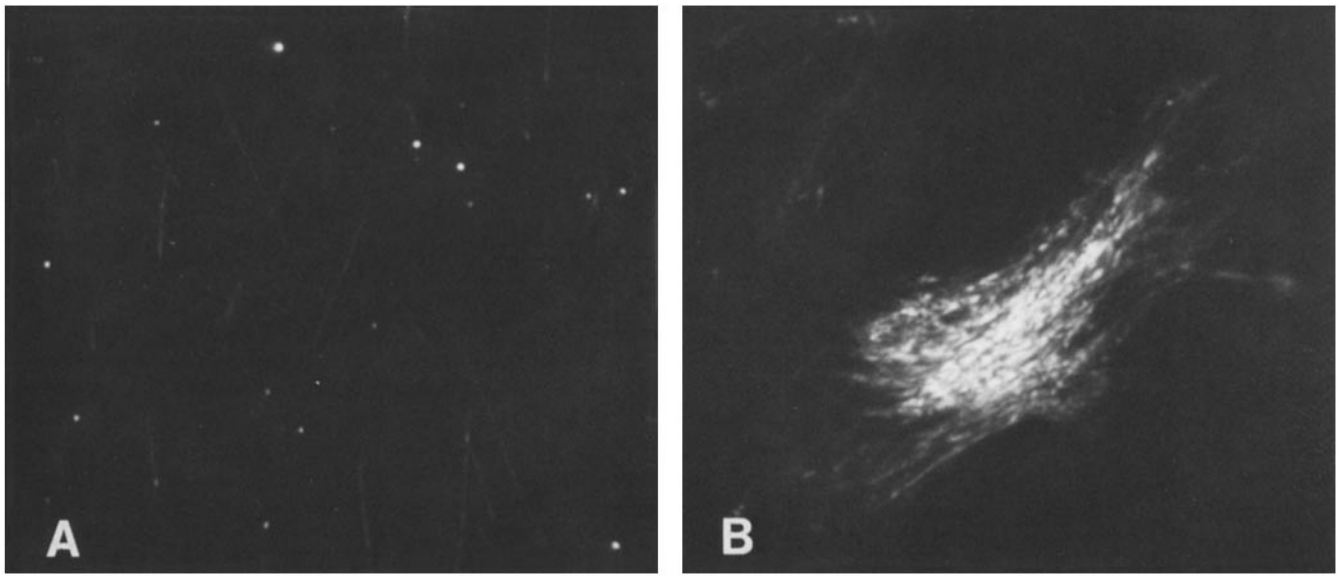

FIGURE 3 Darkfield microscopy shows the bundling of microtubules produced by incubation with cytoplasmic dynein-like ATPase. MAP-free microtubules diluted to 0.2 mg/ml with PME are shown in *A*. In *B*, the microtubules have been diluted to the same concentration with cytoplasmic dynein-like ATPase prepared by microtubule affinity and ATP-induced release. Nearly all of the microtubules are gathered into large bright bundles. × 1,000.

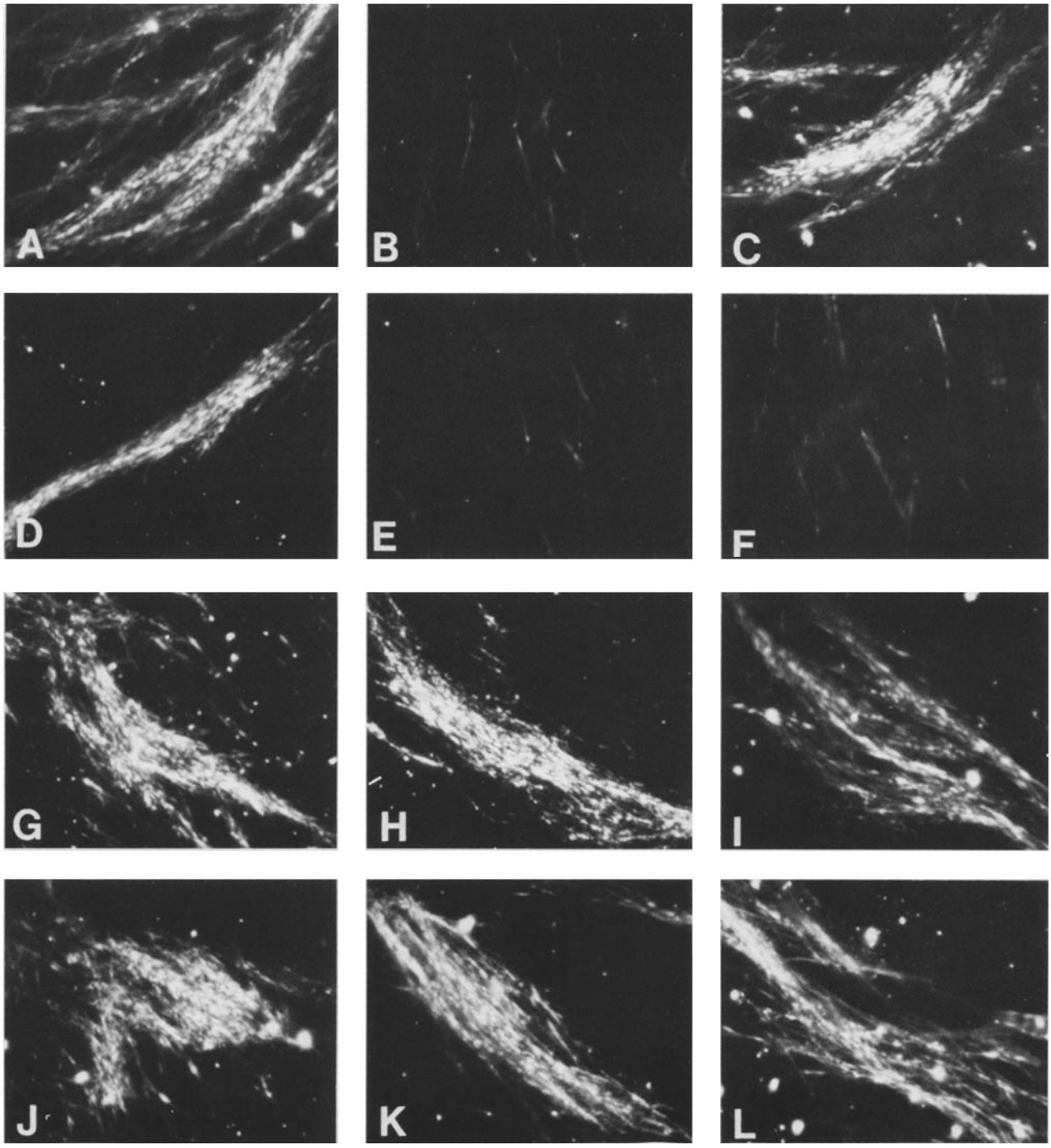

FIGURE 4 Darkfield microscopy reveals the effects of four nucleotide treatments on microtubule bundling induced by cytoplasmic dynein-like ATPase. Bundled microtubules (*A*) are dispersed at 5 min after ATP addition (*B*); after 30 min they are again bundled together (*C*). Bundles (*D*) are also dispersed by ATP plus vanadate after 5 min (*E*), but fail to reassociate after 60 min (*F*). Bundles (*G*) are not appreciably dispersed by ATPγS after 5 min (*H*) or 30 min (*I*). Bundles (*J*) are also not noticeably dispersed by addition of AMP-PNP after 5 min (*K*) or 30 min (*L*). × 800.

plasm? and second, does it interact with microtubules in the manner expected for dynein? In this study, we have addressed these questions using several different techniques.

We have developed an enrichment scheme for dynein-like ATPase from the sea urchin egg that exploits its size and microtubule-binding properties. We recovered an ATPase fraction that was dynein-like by the criteria outlined by Gibbons et al. (14)—it contained a MgATPase with a high molecular weight and gel bands in the 300,000-mol-wt range. In in vitro assays, the sizing column-enriched ATPase fraction showed a ratio of Mg- to Ca-stimulation (1.2) and an ATP specificity similar to axonemal dyneins. It was unlike mitochondrial or Na/K ATPases in showing no inhibition by oligomycin or ouabain. In addition, we found the cytoplasmic ATPase to be dynein-like and not myosin-like by virtue of complete lack of K/EDTA-stimulated ATPase activity. Fur-

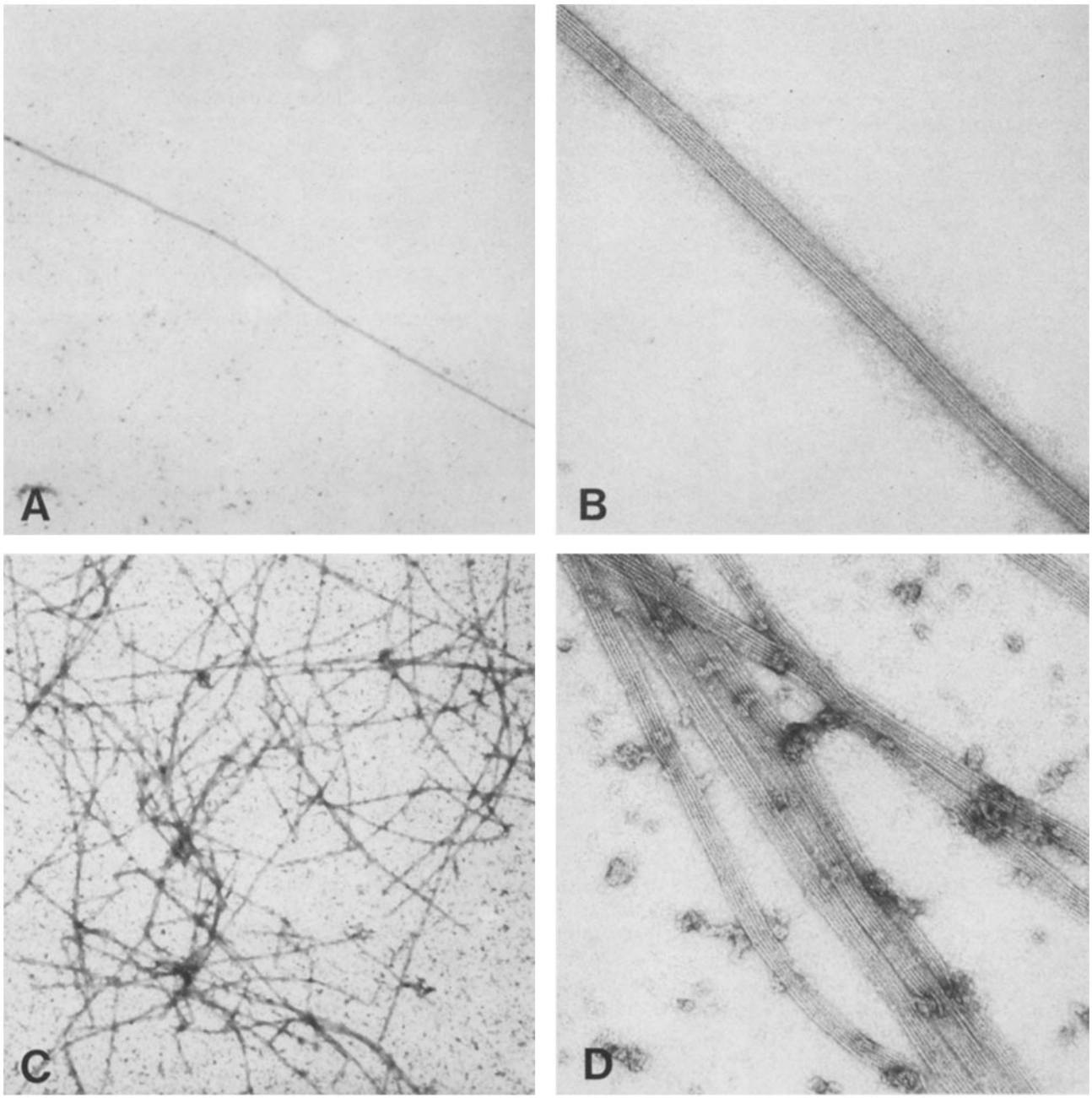

FIGURE 5 Negative stain electron microscopy of dark-field incubation mixtures. Microtubules alone: typical views are shown in *A* and *B*. Microtubles plus cytoplasmic dynein-like ATPase are shown in *C* and *D*. × 20,000 (*A* and *C*); × 160,000 (*B* and *D*).

thermore, this MgATPase activity was inhibited by EHNA in the same range (1–2 mM) as axonemal dyneins, and, like those dyneins, was highly sensitive to vanadate (1–2 μM). Although the inhibitor data and Eadie-Hofstee plots suggested that there was only one ATPase in this preparation, we cannot completely rule out the possibility that it contained more than one.

Another characteristic we expect of dynein, and an essential one if it is to play a role in force generation, is the ability to bind to and cross-link microtubules. We assessed this capacity in three ways, the first of which was the pelleting binding assay. Here we found that sizing column-enriched MgATPase activity pelleted with MAP-free microtubules through a sucrose pad in the presence of Mg^{++}. This, considered along with the 75% reduction in pelleting ATPase activity in the absence of Mg^{++}, indicated that the ATPase had a Mg-dependent interaction with microtubules. The pelleting assay also showed that the binding was ATP sensitive; inclusion of 0.5 mM ATP in the assay reduced the pelleting ATPase activity by >50%. This was similar to the findings of Mitchell and Warner (29) for dynein-B subfiber interactions in *Tetrahymena* ciliary axonemes. Furthermore, it suggested that the ATPase could be further purified from the enriched column peak by microtubule affinity and ATP-induced release.

This proved to be possible. When the peak MgATPase fractions from the sizing column were dialyzed, clarified, and incubated with taxol-polymerized microtubules, and the microtubules were pelleted, 75% of the MgATPase activity pelleted with them. When these pellets were extracted with 2 mM MgATP, they released 25–35% of the activity to the

supernatant. Viewed on 4–8% gradient SDS polyacrylamide gels, this supernatant showed four major peptides in addition to tubulin extracted from the microtubules (Fig. 1*D*). As described in Results, these polypeptides had M_r values of 295,000, 246,000, 243,000, and 180,000. This was consistent with the complex polypeptide composition of axonemal dyneins such as the 21S urchin flagellar dynein 1, which has several peptides that fall into three size classes (53). Although the M_r of 295,000 is less than reported values for the high molecular weight bands of axonemal dyneins, in our gel system axonemal peptides from *S. purpuratus* sperm tails and *Tetrahymena* cilia also migrate in the 295,000–300,000-mol-wt region (data not shown). The estimated specific activity of the nontubulin peptides of the affinity-purified ATPase preparation of 0.850 μmol P_i/min per protein was similar to the values obtained for dynein-like ATPase prepared by Hisanaga and Sakai from a different species (21, 22). We will refer to our microtubule affinity/ATP-released ATPase fraction as cytoplasmic dynein-like ATPase.

By its design, our purification procedure provided us with a protein that was dynein-like, having the appropriate ATPase activity, size, and ATP-sensitive microtubule binding characteristics. Using this microtubule affinity-purified ATPase, we wanted to assess its capacity to cross-link microtubules and to relate its cross-linking properties to its ATPase activity. To this end we employed dark-field optics, which allowed us to observe a very large population of microtubules under various conditions while retaining the ability to resolve individual microtubules.

When the ATPase was added to MAP-free taxol-polymerized brain microtubules, virtually all of the microtubules were gathered into bundles (Fig. 3). This suggested that the ATPase did in fact have the capacity to cross-link microtubules. To relate this cross-linking capacity to the ATPase activity, we added ATP, ATP + vanadate, ATPγS, or AMP-PNP to these bundled microtubules. Addition of ATP or ATP plus vanadate caused complete dispersal of the bundles to individual microtubules, indicating detachment of the cross-linking element (Fig. 4, *B* and *E*). This was consistent with results obtained with axonemal dynein in intact axonemes, decorated outer doublets and brain microtubule, and trypsin-digested axonemes, where ATP addition results in the detachment of rigor bound dynein arms from microtubules and this detachment is not prevented by vanadate (41, 43, 49). If, after dispersing the bundles with ATP, we allowed sufficient time for the ATPase to hydrolyze the nucleotide, the microtubules formed bundles again (Fig. 4*C*). However, in samples dispersed by ATP plus sufficient vanadate to inhibit ATPase activity, microtubules failed to form bundles again (Fig. 4*F*). This too is consistent with results obtained for axonemal dynein decoration of doublet and brain microtubules (43, 49) where rebinding after ATP-induced release was blocked by vanadate. In the axonemal system, ATP-induced release and the coupling of hydrolysis and product release to dynein reattachment are presumed to be part of the mechanochemical cross-bridge cycle; we do not know what role they may play for cytoplasmic dynein-like ATPase.

When we added the nonhydrolyzable ATP analogues ATPγS or AMP-PNP to bundled microtubules, we observed little if any release of bundling. This suggested that either these analogues bind to the ATPase very poorly or that hydrolysis is necessary for release. It should be noted that our ATP-vanadate result does not rule out the latter possibility, since vanadate apparently does not inhibit initial hydrolysis, but rather binds to an enzyme product complex, preventing product release (13, 15, 23, 41, 46, 47). In fact, Penningroth et al. (35) have obtained evidence that ATP hydrolysis is necessary for relaxation of rigor axonemes.

Recent evidence suggests that the binding of MAP2 to microtubules is inhibited by phosphorylation (5). Our result with ATPγS makes it unlikely that phosphorylation is responsible for the release seen here. Although ATPγS is not hydrolyzed by ATPases it serves as a good substrate for kinases, producing irreversible thiophosphorylation (16).

To further compare cytoplasmic dynein-like ATPase with axonemal dynein, we prepared samples from the dark-field assay for negative stain electron microscopy. In samples of microtubules bundled by the ATPase, we observed extensive close association of microtubules (Fig. 5). However, we observed no stretches of obvious periodic bridges, and there may have been two reasons for this. First, because of material limitations, the ratio of ATPase to tubulin was only around one-third of that used to saturate microtubules with axonemal dynein decoration (18, 19, 43). This may have precluded seeing periodic decoration. A second possibility is that sea urchin cytoplasmic ATPase is difficult to preserve for electron microscopy. This would be consistent with our experience with sea urchin flagellar dynein, which gave poor decoration even when ATPase assays indicated that the microtubules were saturated with dynein (unpublished data). By scaling up our purification procedure and trying different methods of sample preparation, we hope to overcome these difficulties.

To conclude, we return to the two questions posed at the beginning of this discussion. First, concerning whether there is an ATPase in the cytoplasm that resembles dynein, we have shown that there is an ATPase in sea urchin eggs that shares a number of characteristics with axonemal dynein. Its size, complex polypeptide composition, cationic requirements, and sensitivity to inhibitors are strikingly similar to the axonemal ATPase. As for the question of its microtubule interactions, we have shown that the cytoplasmic ATPase binds to microtubules in a Mg-dependent, ATP-sensitive manner. Furthermore, as judged by the dark-field assay, it mediates an interaction between microtubules that is related to ATP binding and hydrolysis in precisely the manner demonstrated for axonemal dynein.

We suggest that cytoplasmic dynein-like ATPase is a good candidate for the force-generating element in microtubule-based intracellular movements. It not only possesses the necessary microtubule-binding characteristics, but also shows inhibition by EHNA and vanadate which closely matches their inhibition of anaphase B in permeabilized cell models (6, 7), of pronucleus migration in fertilized sea urchin eggs (44), and of particle movements in axons (11), erythrophores (1), and permeabilized fibroblasts (10) and melanophores (8). To relate the observed properties of cytoplasmic dynein-like ATPase to its potential function in vivo, we would like to know if it can generate force between microtubules. To this end, we are using dark-field microscopy to observe whether microtubules slide over each other during the formation and ATP-induced release of microtubules bundled by the ATPase.

We wish to thank Drs. David Asai, Kent McDonald, Stephen Penningroth, and Richard Vallee for helpful discussions. We are also grateful to Susan Elliger for technical assistance.

This work was supported by National Institute of Health grant

GM23238 to W. Z. Cande. P. J. Hollenbeck was supported by a National Science Foundation predoctoral fellowship.

Received for publication 19 September 1983, and in revised form 12 June 1984.

REFERENCES

1. Beckerle, M. C., and K. R. Porter. 1982. Inhibitors of dynein block intracellular transport in erythrophores. *Nature (Lond.).* 295:701–703.
2. Bloodgood, R. A. 1975. Biochemical analysis of axostyle motility. *Cytobios.* 14:101–120.
3. Bloodgood, R. A., and K. R. Miller. 1974. Freeze fracture of microtubules and bridges in motile axostyles. *J. Cell Biol.* 62:660–671.
4. Bradford, M. M. 1976. A rapid and sensitive method for the quantitation of microgram quantities of protein utilizing the principle of protein-dye binding. *Anal. Biochem.* 72:248–254.
5. Burns, R. G., K. Islam, and R. Chapman. 1983. The graduated phosphorylation of MAP2 regulates the MAP2:microtubule interaction. *J. Cell Biol.* 97(5, pt. 2):200*a*. (Abstr.)
6. Cande, W. Z. 1982. Inhibition of spindle elongation in permeabilized cells by erythro-9[3-(2-hydroxynonyl)] adenine. *Nature (Lond.).* 295:700–701.
7. Cande, W. Z. 1982. Nucleotide requirements for anaphase chromosome movements in permeabilized mitotic cells: anaphase B but not anaphase A requires ATP. *Cell.* 28:15–22.
8. Clark, T. G., and J. L. Rosenbaum. 1982. Pigment particle translocation in detergent permeabilized melanophores of Fundulus heteroclitus. *Proc. Natl. Acad. Sci. USA.* 79:4655–4659.
9. Fiske, C. H., and Y. Subbarow. 1925. The colorimetric determination of phosphorus. *J. Biol. Chem.* 66:375–400.
10. Forman, D. S. 1982. Vanadate inhibits saltatory organelle movement in a permeabilized cell model. *Exp. Cell Res.* 141:139–147.
11. Forman, D. S., K. J. Brown, and D. R. Livengood. 1983. Fast axonal transport in permeabilized lobster giant axons is inhibited by vanadate. *J. Neurosci.* 3:1279–1288.
12. Gibbons, B. H., and I. R. Gibbons. 1976. Functional recombination of dynein 1 with demembranated sea urchin sperm partially extracted with KCl. *Biochem. Biophys. Res. Commun.* 73:1–6.
13. Gibbons, I. R., M. P. Cosson, J. A. Evans, B. H. Gibbons, B. Houck, K. H. Martinson, W. S. Sale, and W. Y. Tang. 1978. Potent inhibition of dynein adenosinetriphosphatase and of the motility of cilia and sperm flagella by vanadate. *Proc. Natl. Acad. Sci. USA.* 75:2220–2224.
14. Gibbons, I. R., E. Fronk, B. H. Gibbons, and K. Ogawa. 1976. Multiple forms of dynein in sea urchin sperm flagella. *Cold Spring Harbor Conf. Cell Prolif.* 3(Book A):915–932.
15. Goodno, C. C. 1979. Inhibition of myosin ATPase by vanadate ion. *Proc. Natl. Acad. Sci. USA* 76:2620–2624.
16. Gratecos, D., and E. H. Fischer. 1974. Adenosine 5′-0(3-thiotriphosphate) in the control of phosphorylase activity. *Biochem. Biophys. Res. Commun.* 58:960–7.
17. Grimstone, A. V., and L. R. Cleveland. 1965. The fine structure and function of the contractile axostyles of certain flagellates. *J. Cell Biol.* 24:387–400.
18. Haimo, L. T., and B. R. Telzer. 1981. Dynein-microtubule interactions: ATP-sensitive dynein binding and the structural polarity of mitotic microtubules. *Cold Spring Harbor Symp. Quant. Biol.* 46:207–217.
19. Haimo, L. T., B. R. Telzer, and J. L. Rosenbaum. 1979. Dynein binds to and cross-bridges cytoplasmic microtubules. *Proc. Natl. Acad. Sci. USA.* 76:5759–5763.
20. Hepler, P. K., J. R. McIntosh, and S. Cleveland. 1970. Intermicrotubule bridges in mitotic spindle apparatus. *J. Cell Biol.* 45:438–444.
21. Hisanaga, S. I., and H. Sakai. 1980. Cytoplasmic dynein of the sea urchin egg: a partial purification and characterization. *Dev. Growth Differ.* 22:373–384.
22. Hisanaga, S. I., and H. Sakai. 1983. Cytoplasmic dynein of the sea urchin egg. II. Purification, characterization, and interaction with microtubules and Ca-calmodulin. *J. Biochem. (Tokyo).* 93:87–98.
23. Kobayashi, T., T. Martensen, J. Nath, and M. Flavin. 1978. Inhibition of dynein ATPase by vanadate, and its possible use as a probe for the role of dynein in cytoplasmic motility. *Biochem. Biophys. Res. Commun.* 81:1313–1318.
24. Laemmli, U. K. 1970. Cleavage of structural proteins during the assembly of the head of bacteriophage T4. *Nature (Lond.).* 227–680–685.
25. Langford, G. M. 1984. Length and appearance of projections on neuronal microtubules in vitro after negative staining: evidence against a crosslinking function for MAPs. *J. Ultrastruct. Res.* 85:1–10.
26. Mazia, D., R. R. Chaffee, and R. M. Iverson. 1961. Adenosine triphosphatase in the mitotic apparatus. *Proc. Natl. Acad. Sci. USA.* 47:788–790.
27. McDonald, K. L., M. K. Edwards, and J. R. McIntosh. 1979. Cross-sectional structure of the central mitotic spindle of *Diatoma vulgare*: evidence for specific interactions between antiparallel microtubules. *J. Cell Biol.* 83:443–461.
28. McDonald, K. L., J. R. McIntosh, and D. H. Tippit. 1977. On the mechanism of anaphase spindle elongation in *Diatoma vulgare*. *J. Cell Biol.* 74:377–388.
29. Mitchell, D. R., and F. D. Warner. 1980. Interactions of dynein arms with B subfibers of *Tetrahymena* cilia: quantitation of the effects of magnesium and adenosine triphosphate. *J. Cell Biol.* 87:84–97.
30. Murofushi, H., Y. Minami, G. Matsumoto, and H. Sakai. 1983. Bundling of microtubules *in vitro* by a high molecular weight protein prepared from the squid axon. *J. Biochem. (Tokyo).* 93:639–650.
31. Murphy, D. B., and G. G. Borisy. 1975. Association of high-molecular-weight proteins with microtubules and their role in microtubule assembly in vitro. *Proc. Natl. Acad. Sci. USA.* 72:2696–2700.
32. Pallini, V., C. Mencarelli, L. Bracci, M. Contorni, P. Ruggiero, A. Tiezzi, and R. Manetti. 1983. Cytoplasmic nucleoside-triphosphatases similar to axonemal dynein can occur widely in different cell types. *J. Submicrosc. Cytol.* 15:229–235.
33. Penningroth, S. M., and A. Cheung. 1983. Erythro-9-[3-(2-hydroxynonyl)] adenine (EHNA): a new link between cytoplasmic and axonemal dyneins. *J. Submicrosc. Cytol.* 15:223–227.
34. Penningroth, S. M., A. Cheung, P. Bouchard, C. Gagnon, and C. W. Bardin. 1982. Dynein ATPase is inhibited selectively *in vitro* by erythro-9-[3-(2-hydroxynonyl)] adenine. *Biochem. Biophys. Res. Commun.* 104:234–240.
35. Penningroth, S. M., A. Cheung, K. Olehnik, and R. Koslosky. 1982. Mechanochemical coupling in the relaxation of rigor wave sea urchin sperm flagella. *J. Cell Biol.* 92:733–41.
36. Pratt, M. M. 1979. Comparison of flagellar and egg dynein. *J. Cell Biol.* 83(2, Pt. 2): 350*a*. (Abstr.)
37. Pratt, M. M. 1980. The identification of a dynein ATPase in unfertilized sea urchin eggs. *Dev. Biol.* 74:364–378.
38. Pratt, M. M., Otter, T., and E. D. Salmon. 1980. Dynein-like Mg^+ ATPase in mitotic spindles isolated from sea urchin embryos (*Strongylocentrotus droebachiensis*). *J. Cell Biol.* 86:738–745.
39. Pratt, M. M., and R. Stephens. 1978. Dynein synthesis in sea urchin embryos. *J. Cell Biol.* 79(2, Pt. 2):300*a*. (Abstr.)
40. Sakai, H. 1978. The isolated mitotic apparatus and chromosome motion. *Int. Rev. Cytol.* 55:23–48.
41. Sale, W. S., and I. R. Gibbons. 1979. Study of the mechanism of vanadate inhibition of the dynein cross-bridge cycle in sea urchin sperm flagella. *J. Cell Biol.* 82:291–298.
42. Satir, P. 1979. Basis of flagellar motility in spermatozoa: current status. *In* The Spermatozoon: Maturation, Motility, and Surface Properties. D. W. Fawcett and J. M. Bedford, editors. Urban and Scharzenberg, Baltimore. 81–90.
43. Satir, P., J. Wais-Steider, S. Lebduska, A. Nasr, and J. Avolio. 1981. The mechanochemical cycle of the dynein arm. *Cell Motility.* 1:303–327.
44. Schatten, G., R. Balczon, C. Cline, and H. Schatten. 1982. EHNA, a dynein inhibitor, blocks the nuclear movements during sea urchin fertilization. *J. Cell Biol.* 95(2, Pt. 2):166*a*. (Abstr.)
45. Shelanski, M. L., F. Gaskin, and R. Cantor. 1973. Microtubule assembly in the absence of added nucleotides. *Proc. Natl. Acad. Sci. USA.* 70:765–768.
46. Shimizu, T. 1981. Steady-state kinetic study of vanadate-induced inhibition of dynein adenosine triphosphatase activity from *Tetrahymena*. *Biochemistry.* 20:4347–4354.
47. Shimizu, T., and K. A. Johnson. 1983. Presteady state kinetic analysis of vanadate-induced inhibition of the dynein ATPase. *J. Biol. Chem.* 258:13833–13840.
48. Summers, K. E., and I. R. Gibbons. 1973. Effects of trypsin digestion of flagellar structures and their relationship to motility. *J. Cell Biol.* 58:618–629.
49. Takahashi, M., and Y. Tonomura. 1978. Binding of the 30S dynein with the B-tubule of the outer doublet of axonemes from *Tetrahymena pyriformis* and adenosine triphosphate-induced dissociation of the complex. *J. Biochem. (Tokyo).* 84:1339–1355.
50. Tilney, L. G. 1971. How microtubule patterns are generated. The relative importance of nucleation and bridging of microtubules in the formation of the axoneme of *Radiophrys*. *J. Cell Biol.* 51:837–854.
51. Tucker, J. B. 1968. Fine structure and function of the cytopharyngeal basket in the ciliate *Nassula*. *J. Cell Sci.* 3:493–514.
52. Warner, F. D. 1978. Cation-induced attachment of ciliary dynein cross-bridges. *J. Cell Biol.* 77:R19–R26.
53. Warner, F. D. 1980. Dynein: the mechanochemical coupling adenosine triphosphatase of microtubule-based sliding filament mechanisms. *Int. Rev. Cytol.* 66:1–43.
54. Warner, F. D., and D. R. Mitchell. 1981. Polarity of dynein-microtubule interactions in vitro: cross-bridging between parallel and antiparallel microtubules. *J. Cell Biol.* 89:35–44.
55. Weisenberg, R. C., and E. W. Taylor. 1968. Studies on ATPase activity of sea urchin eggs and the isolated mitotic apparatus. *Exp. Cell Res.* 53:372–384.
56. Zanetti, N. C., D. R. Mitchell, and F. D. Warner. 1979. Effects of divalent cations on dynein cross-bridging and ciliary dynein sliding. *J. Cell Biol.* 80:573–588.